PROCEEDINGS OF SCIENCE

Probing the nature of electroweak symmetry breaking with Higgs boson pairs in ATLAS

Ang LI[a,1,*], **On behalf of ATLAS Collaboration,**
[a] *Physics Department, Brookhaven National Laboratory, USA*
E-mail: ang.l@cern.ch

In the Standard Model, the Higgs field acquires a non-zero vacuum expectation value, breaking electroweak symmetry and giving mass to fundamental particles. The Higgs boson self-coupling, precisely predicted by the Standard Model, defines the shape of the Higgs potential and can be probed through rare Higgs boson pair (HH) production at the LHC. This contribution presents the latest HH searches by the ATLAS experiment using the full Run 2 dataset at $\sqrt{s} = 13$ TeV. These non-resonant searches test the Standard Model and constrain both the Higgs self-coupling and the quartic $VVHH$ coupling. A combined analysis of different HH decay yields the best current precision. Finally, projections for the High Luminosity LHC (HL-LHC) show that increased luminosity will further improve the sensitivity and precision of HH measurements.

The 43rd International Symposium on Physics in Collision (PIC2024)
22–25 October 2024
Athens, Greece
*Speaker

© Copyright owned by the author(s) under the terms of the Creative Commons Attribution-NonCommercial-NoDerivatives 4.0 International License (CC BY-NC-ND 4.0) All rights for text and data mining, AI training, and similar technologies for commercial purposes, are reserved. ISSN 1824-8039 . Published by SISSA Medialab.

PoS(PIC2024)012

1. Introduction

Since the Higgs boson's discovery at the LHC in 2012 [1, 2], a key goal of ATLAS [3] and CMS [4] has been to measure its properties and couplings with increasing precision. Among these properties, the Higgs boson's self-coupling (λ_{HHH}) is particularly important, as it determines the shape of the Higgs potential and underpins the mechanism of electroweak symmetry breaking. The production of Higgs boson pairs (HH) provides a direct way to probe this self-coupling. In the Standard Model (SM), HH production is dominated by gluon-gluon fusion (ggF). Despite this, the HH production cross section is much smaller than that of single Higgs production [5]. The next most significant mechanism is vector-boson fusion (VBF).

To quantify the rate of HH production relative to the SM expectation, a signal strength parameter μ_{HH} is defined as: $\mu_{HH} = \frac{\sigma_{HH}}{\sigma_{HH}^{\mathrm{SM}}}$, where σ_{HH} is the measured cross section and $\sigma_{HH}^{\mathrm{SM}}$ is the SM prediction. A value of $\mu_{HH} = 1$ corresponds to the SM rate, while deviations from unity suggest new physics. In addition, two parameters are commonly introduced to describe deviations in the Higgs self-coupling and related interactions: $\kappa_\lambda = \frac{\lambda_3}{\lambda_3^{\mathrm{SM}}}$ and $\kappa_{2V} = \frac{\lambda_{VVHH}}{\lambda_{VVHH}^{\mathrm{SM}}}$, where λ_3 is the trilinear Higgs self-coupling and λ_{VVHH} characterizes the $HHVV$ interaction. In the SM, both κ_λ and κ_{2V} are equal to one, and any deviation from these values would indicate possible new physics beyond the Standard Model.

2. Overview of Di-Higgs Decay Channels

$HH \to b\bar{b}\gamma\gamma$

The $HH \to b\bar{b}\gamma\gamma$ channel [6] has a small branching ratio but a very clean signature, benefiting from excellent diphoton ($m_{\gamma\gamma}$) mass resolution and low background. The final state consists of two b-jets and two photons, with the diphoton invariant mass required to be 105 GeV $< m_{\gamma\gamma} <$ 160 GeV. Events are categorized into a high-mass category ($m^{\star}_{b\bar{b}\gamma\gamma} > 350$ GeV) and a low-mass category ($m^{\star}_{b\bar{b}\gamma\gamma} < 350$ GeV), where $m^{\star}_{b\bar{b}\gamma\gamma} = m_{b\bar{b}\gamma\gamma} + (125\ \mathrm{GeV} - m_{b\bar{b}}) + (125\ \mathrm{GeV} - m_{\gamma\gamma})$. Within each mass category, a Boosted Decision Tree (BDT) is trained, and its output is used to define further sub-categories (four for low mass and three for high mass). Although no dedicated VBF category is defined, the mass and pseudorapidity separation ($\Delta\eta$) of VBF-tagged jets are included as inputs to the BDTs. A fit to $m_{\gamma\gamma}$ is performed in each of the seven categories. The $\gamma\gamma$-continuum background is modeled by an exponential fit in the sidebands, while signal and single-Higgs backgrounds are modeled by a double-sided Crystal Ball function. At the 95% confidence level, the observed (expected) upper limit on the signal strength is $\mu_{HH} < 4.0$ (5.0); for κ_λ, the observed (expected) range is $[-1.4, 6.9]$ ($[-2.8, 7.8]$), and for κ_{2V}, it is $[-0.5, 2.7]$ ($[-1.1, 3.3]$).

$HH \to b\bar{b}\tau^+\tau^-$

The $HH \to b\bar{b}\tau^+\tau^-$ analysis [7] considers two main τ-lepton decay channels: the fully hadronic channel ($\tau_{\mathrm{had}}\tau_{\mathrm{had}}$) and the lepton-hadron channel ($\tau_\ell\tau_{\mathrm{had}}$), where one τ decays leptonically. The $\tau_\ell\tau_{\mathrm{had}}$ channel is further split based on the trigger into SLT (Single Lepton Trigger) and LTT (Lepton + $\tau_{\text{had-vis}}$ triggers), resulting in three final-state categories. A BDT is used in each final-state category to separate ggF and VBF production. For ggF production, events are further divided

PoS(PIC2024)012

into a low-mass category ($m_{HH} < 350$ GeV) and a high-mass category ($m_{HH} > 350$ GeV). One control region, defined by $m_{\ell\ell}$, is used, and a BDT is trained in each signal region to discriminate signal from background. The main background arises from fake τ candidates in $t\bar{t}$ and multijet processes, estimated using data-driven methods with fake factors derived from control regions. At the 95% confidence level, the observed (expected) upper limit on the signal strength is $\mu_{HH} < 5.9$ (3.3); for κ_λ, the observed (expected) range is $[-3.1, 9.0]$ ($[-2.5, 9.3]$), and for κ_{2V}, it is $[-0.5, 2.7]$ ($[-0.2, 2.4]$). Among the considered channels, the hadronic ($\tau_{\text{had}}\tau_{\text{had}}$) channel is the most sensitive, and overall, $HH \to b\bar{b}\tau^+\tau^-$ is expected to provide the greatest sensitivity to SM di-Higgs production.

$HH \to b\bar{b}b\bar{b}$

The $HH \to b\bar{b}b\bar{b}$ channel has been studied in two distinct analyses. In the resolved analysis [8], events are characterized by four b-tagged jets. The closest jet pairs are combined to form Higgs candidates, and events are classified into ggF and VBF categories. In the boosted analysis [9], events consist of two large-radius jets from $X \to bb$ decays and two VBF jets, with only the VBF topology considered. The signal is localized in the m_{H_1} vs. m_{H_2} plane. The main background comes from QCD multijet events; its normalization is determined from sidebands in the signal region, and a scale factor obtained from a neural network is applied in both the resolved and boosted categories. The m_{HH} distribution is fitted using a BDT approach in both categories. At the 95% confidence level, the observed (expected) upper limit on the signal strength in the resolved category is $\mu_{HH} < 5.4$ (8.1); for κ_λ, the observed (expected) range is $-3.5 < \kappa_\lambda < 11.3$ ($-5.4 < \kappa_\lambda < 11.4$). Combining resolved and boosted categories, the observed (expected) range for κ_{2V} is $0.55 < \kappa_{2V} < 1.49$ ($0.37 < \kappa_{2V} < 1.67$).

$HH \to 2b + 2\ell + E_{\mathbf{T}}^{\mathbf{miss}}$

The $HH \to 2b{+}2\ell{+}E_{\text{T}}^{\text{miss}}$ channel [10] considers decays where one Higgs boson goes to $b\bar{b}$ while the other decays into W^+W^-, $\tau^+\tau^-$, or ZZ, leading to a final state with leptons and neutrinos ($\ell = e, \mu$). The leptons have opposite charges and may be of different flavors. The signal and control regions are defined based on $m_{\ell\ell}$ and m_{bb}. A fit is performed using the five (seven) highest BDT (DNN) bins in the VBF (ggF) topology. At the 95% confidence level, the observed (expected) upper limit on the signal strength is $\mu_{HH} < 9.7$ (16.3); for κ_λ, the observed (expected) range is $-6.2 < \kappa_\lambda < 13.3$ ($-8.1 < \kappa_\lambda < 15.5$), and for κ_{2V}, it is $-0.17 < \kappa_{2V} < 2.4$ ($-0.51 < \kappa_{2V} < 2.7$).

$HH \to$ Multi-leptons

This multi-lepton analysis [11] considers nine different di-Higgs decay final states, covering a variety of channels with different numbers of hadronic taus, light leptons, and photons. A BDT is trained in each sub-channel, and its discriminant is used in the multilepton channels. Categories are defined based on $m_{\gamma\gamma}$ for the combined $\gamma\gamma$ and multilepton channels. At the 95% confidence level, the observed (expected) upper limit on the signal strength is $\mu_{HH} < 17$ (11); for κ_λ, the observed (expected) range is $-6.2 < \kappa_\lambda < 1.6$ ($-4.5 < \kappa_\lambda < 9.6$), and for κ_{2V}, it is $-2.5 < \kappa_{2V} < 4.6$ ($-1.9 < \kappa_{2V} < 4.1$). No single channel dominates the sensitivity; all channels contribute to achieving the expected limit.

PoS(PIC2024)012

3. Combination

The combined analysis described in Ref. [12] simultaneously fits multiple HH production channels: $HH \to b\bar{b}\gamma\gamma$, $HH \to b\bar{b}\tau^+\tau^-$, $HH \to b\bar{b}b\bar{b}$, $HH \to 2b + 2\ell + E_{\mathrm{T}}^{\mathrm{miss}}$, and $HH \to$ Multi-leptons final states. Including all these channels together enhances sensitivity to non-resonant HH production.

At the 95% confidence level (CL), this combination sets the observed upper limit on the HH signal strength at $\mu_{HH} < 2.9$, compared to an expected limit of 2.4, as shown in Figure 1.

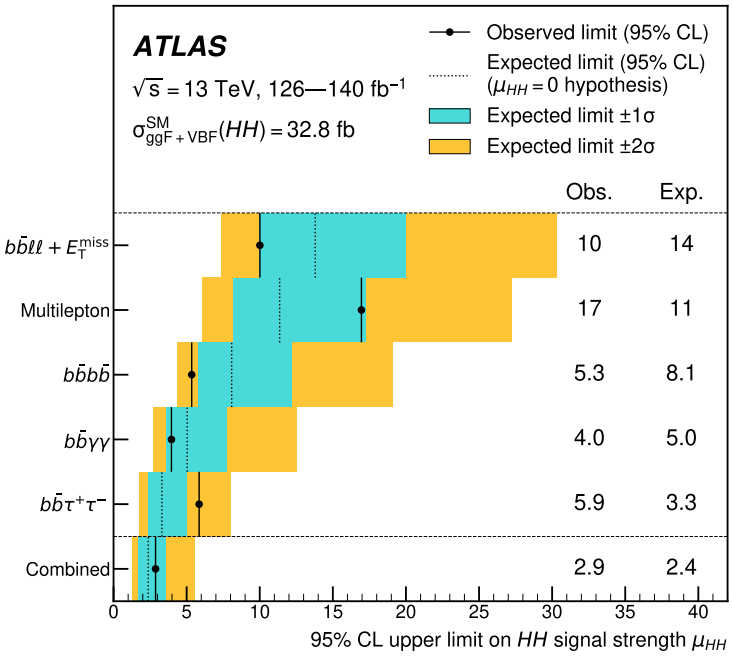

Figure 1: Observed and expected 95% CL upper limits on the HH signal strength μ_{HH}. The shaded bands indicate one- and two-standard-deviation variations of the expected limit. Adapted from Ref. [12].

The analysis also constrains the trilinear Higgs self-coupling parameter κ_λ and the $HHVV$ coupling modifier κ_{2V}. Figure 2 (a) shows the observed and expected intervals for κ_λ, resulting in $-1.2 < \kappa_\lambda < 7.2$ (expected $-1.6 < \kappa_\lambda < 7.2$). Figure 2 (b) provides the corresponding constraints on κ_{2V}, with an observed range of $0.6 < \kappa_{2V} < 1.5$ (expected $0.4 < \kappa_{2V} < 1.6$). These improved constraints highlight the enhanced statistical power and complementary nature of the combined analysis.

4. High Luminosity LHC

The High Luminosity LHC (HL-LHC), scheduled to start in 2030, will run at $\sqrt{s} = 14\,\mathrm{TeV}$ with an integrated luminosity of up to $3000\,\mathrm{fb}^{-1}$. Building on Run 2 experience, the HL-LHC program will increase sensitivity to non-resonant Higgs boson pair (HH) production by combining multiple decay channels [13], including $HH \to b\bar{b}\gamma\gamma$, $HH \to b\bar{b}\tau^+\tau^-$, and $HH \to b\bar{b}b\bar{b}$. With reduced

PoS(PIC2024)012

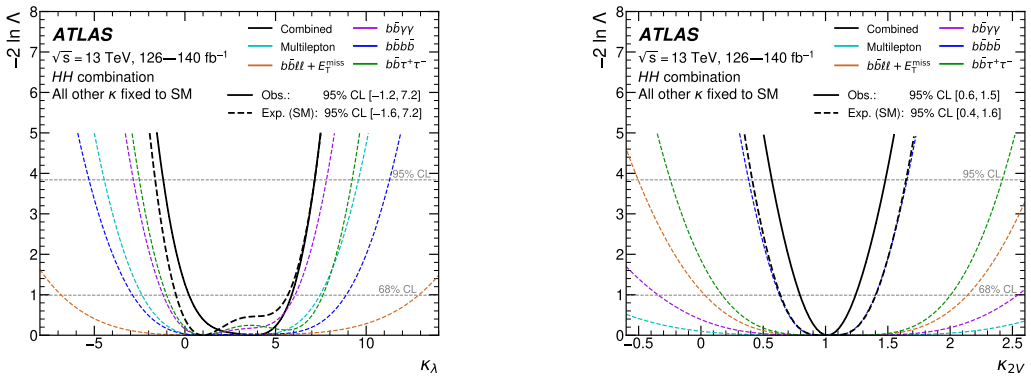

(a) κ_λ constraints **(b)** κ_{2V} constraints

Figure 2: Observed and expected 95% CL intervals on (a) κ_λ and (b) κ_{2V} from the combination analysis. Including all channels improves sensitivity beyond what can be achieved from individual measurements. Adapted from Ref. [12].

theoretical uncertainties and improved b-tagging, the combined HH significance is expected to reach 3.4σ as shown in Figure 3, constraining the Higgs self-coupling κ_λ to $[0.0, 2.5]$ at 95% CL. A

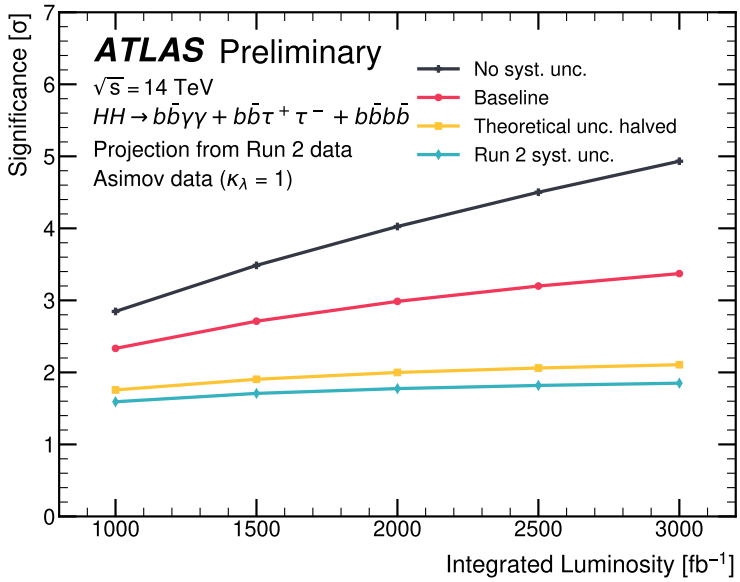

Figure 3: Projected significance of SM Higgs pair production in the $b\bar{b}\gamma\gamma$, $b\bar{b}\tau^+\tau^-$, and $b\bar{b}b\bar{b}$ channels at $\sqrt{s}$ = 14 TeV HL-LHC, for 1000–3000 fb^{-1}. Significance is derived from a signal-plus-background Asimov dataset under the SM hypothesis, assuming four uncertainty scenarios. Adapted from Ref. [13].

dedicated $b\bar{b}\tau^+\tau^-$ study [14], based on Run 2 results, projects a 3.5σ significance (4.6σ statistical only), rising to 3.8σ (4.9σ statistical only) with improved b-tagging. The corresponding 95% CL constraints on κ_λ are $[-0.1, 2.7] \cup [4.5, 6.4]$ with systematics, and $[0.2, 2.1]$ without. These complementary approaches, combining multiple channels and focusing on $b\bar{b}\tau^+\tau^-$, underscore the HL-LHC's potential to probe the Higgs sector and measurements of the Higgs self-coupling.

PoS(PIC2024)012

References

[1] ATLAS Collaboration, *Observation of a new particle in the search for the Standard Model Higgs boson with the ATLAS detector at the LHC*, *Phys. Lett. B* **716** (2012) 1 [1207.7214].

[2] CMS Collaboration, *Observation of a new boson at a mass of 125 GeV with the CMS experiment at the LHC*, *Phys. Lett. B* **716** (2012) 30 [1207.7235].

[3] ATLAS Collaboration, *The ATLAS Experiment at the CERN Large Hadron Collider*, *JINST* **3** (2008) S08003.

[4] CMS Collaboration, *The CMS Experiment at the CERN LHC*, *JINST* **3** (2008) S08004.

[5] LHC Higgs Cross Section Working Group collaboration, *Handbook of LHC Higgs Cross Sections: 4. Deciphering the Nature of the Higgs Sector*, 1610.07922.

[6] ATLAS Collaboration, *Studies of new Higgs boson interactions through nonresonant HH production in the $b\bar{b}\gamma\gamma$ final state in pp collisions at $\sqrt{s}$ = 13 TeV with the ATLAS detector*, *JHEP* **01** (2024) 066 [2310.12301].

[7] ATLAS Collaboration, *Search for the non-resonant production of Higgs boson pairs via gluon fusion and vector-boson fusion in the $b\bar{b}\tau^+\tau^-$ final state in proton–proton collisions at $\sqrt{s}$ = 13 TeV with the ATLAS detector*, *Phys. Rev. D* **110** (2024) 032012 [2404.12660].

[8] ATLAS Collaboration, *Search for nonresonant pair production of Higgs bosons in the $b\bar{b}b\bar{b}$ final state in pp collisions at $\sqrt{s}$ = 13 TeV with the ATLAS detector*, *Phys. Rev. D* **108** (2023) 052003 [2301.03212].

[9] ATLAS Collaboration, *Search for pair production of boosted Higgs bosons via vector-boson fusion in the $b\bar{b}b\bar{b}$ final state using pp collisions at $\sqrt{s}$ = 13 TeV with the ATLAS detector*, 2404.17193.

[10] ATLAS Collaboration, *Search for non-resonant Higgs boson pair production in the $2b + 2\ell + E_T^{miss}$ final state in pp collisions at $\sqrt{s}$ = 13TeV with the ATLAS detector*, *JHEP* **02** (2024) 037 [2310.11286].

[11] ATLAS Collaboration, *Search for non-resonant Higgs boson pair production in final states with leptons, taus, and photons in pp collisions at $\sqrt{s}$ = 13 TeV with the ATLAS detector*, *JHEP* **08** (2024) 164 [2405.20040].

[12] ATLAS Collaboration, *Combination of Searches for Higgs Boson Pair Production in pp Collisions at $\sqrt{s}$ = 13 TeV with the ATLAS detector*, 2406.09971.

[13] ATLAS Collaboration, "HL-LHC prospects for the measurement of Higgs boson pair production in the $b\bar{b}b\bar{b}$ final state and combination with the $b\bar{b}\gamma\gamma$ and $b\bar{b}\tau^+\tau^-$ final states at the ATLAS experiment." ATL-PHYS-PUB-2022-053, 2022, https://cds.cern.ch/record/2841244.

[14] ATLAS Collaboration, "Updated projection of the sensitivity of searches for Higgs boson pair production in the $b\bar{b}\tau^+\tau^-$ final state from LHC Run 2 to the High Luminosity LHC with the ATLAS detector." ATL-PHYS-PUB-2024-016, 2024, https://cds.cern.ch/record/2910850.

PoS(PIC2024)012